Freie Universität Berlin
Department of Physics
Arnimallee 14
14195 Berlin

WS 2011/12

Advanced Lab Course for Master Students
Report

Ma14 - Solid State Laser Principles

Stefanie Kreft
kreft@physik.fu-berlin.de

Samuel Sanchez Viveros
sanchez@physik.fu-berlin.de

November 7, 2011

Tutor: M. Schulze

Contents

1. Theoretical Background

1.1. Laser - Light Amplification by Stimulated Emission of Radiation

In our modern world LASERs are indispensable instruments throughout all branches of high technology industries, research and development. The first LASER was build by Theodore Maiman in 1960. Since then it has been developed from a simple ruby LASER to high specialized devices. The advantages of a LASER are its high coherence length, small beam divergence and its fixed polarization.

1.1.1. Emission and Absorption of Radiation

The light-quantum hypothesis formulated by Einstein in 1905 and his further work published in 1915 were the pathway to understand the properties of light and its interaction with matter of all kinds. In principle there are three important interactions of photons with matter on an atomic scale. Absorption, where an atom absorbs a photon and stores its energy by changing the electronic configuration, and its reverse process, where an excited atom emits an photon and falls back into a state of lower energy. This process is called emission. Emission can happen spontaneously or stimulated by the nearby presence of a photon of suitable energy, i.e. the energy which matches the energy difference between the two involved states (Fig. 1.1). The ratio between the rates at which this processes take place are given by the so called EINSTEIN COEFFICIENTS A_{21}, B_{12} and B_{21}. B_{12} describes absorption, B_{21} stimulated emission and A_{21} spontaneous emission. These coefficients are related via

$$B_{12} = B_{21} = A_{21} \frac{8\pi h\nu^3}{c^3} \,. \tag{1.1.1}$$

The important property of stimulated emission is that the stimulating and stimulated photon have

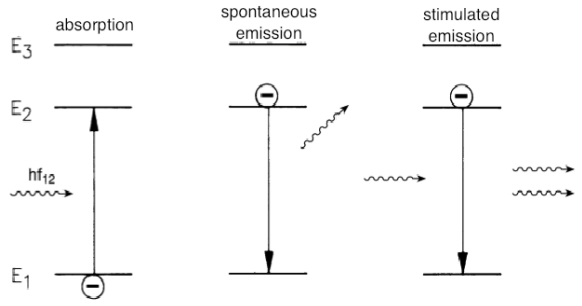

Fig. 1.1.: The three radiation processes. Absorption, spontaneous emission and stimulated emission. (Slightly altered from [1])

identical properties regarding direction of flight, energy, phase and polarization, which account for the overall property of LASER radiation. This leads to an amplification of the intensity of the incoming radiation. However absorption and stimulated emission compete with each other. Taking this into account and adapting Beer-Lambert's law accordingly, yields

$$G = \frac{I}{I_0} = e^{\sigma(N_2 - N_1)d} = e^{gd}, \tag{1.1.2}$$

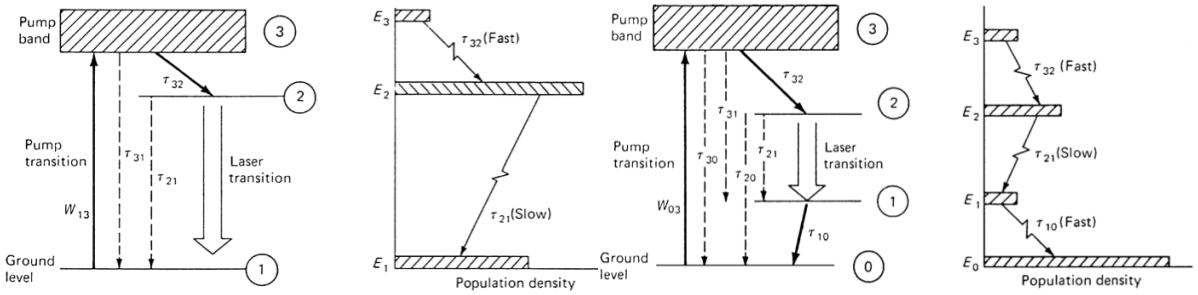

Fig. 1.2.: Simplified term scheme of a three (*l.*) and four level LASER (*r.*). [2]

where σ is the cross section, N_1 the occupation number of the lower and N_2 of the higher energy level and d the relevant length of the system (e.g. the length of an active medium) [1]. Note that due to (1.1.1) the cross section of absorption and stimulated emission are identical. This shows that an amplification is only gained for an inversion of occupation numbers, i.e. $N_2 > N_1$. However, in thermal equilibrium the occupation number of the groundstate is higher than of any excited state because thermal energy at room temperature is small in comparison to excitation energy. Even for infinite high temperatures thermal excitations are restricted to $N_2 = N_1$ due to Boltzman's law. Therefore the inversion of occupation numbers is only achieved by *pumping* the system. The mechanism of pumping is explained in 1.1.2. Due to the distribution of occupation numbers according to Boltzman's law any inversion of a two level system would relax in a very short time. Thus, to establish a stable inversion a system of a minimum of three states is needed to prevent the excited state from immediate relaxation.

1.1.2. Pumping, Lasing, Cavities and Laser Threshold

An active LASER medium, i.e. the medium in which the radiation processes occur, can be pumped by different means. However, in the case of SOLID STATE LASERS only optical pumping is of importance. In the process of optical pumping the active medium is exposed to radiation of appropriate wavelength, which is often in the range of visible light. Suitable pumping light sources are flash or arc lamps or other LASERs (e.g. LASER diodes). The pumping radiation excites electrons from the ground level to an energetically higher level (pump band), whereby the wavelength of the pumping radiation is determined by the energy difference between these two levels. The pump band levels have a short life time and undergo a radiation free transition into the upper LASER level. The energy difference is released in form of thermal energy (phonons in a lattice or kinetic energy in gases respectively). The upper LASER level is characterized by an comparatively long life time, which allows high inversions. Depending on system the LASER transition takes place directly into the ground level (three level system) or into a intermediate level with short life time (four level system) (cf. Fig. 1.2). The advantage of the four level system is that the needed inversion is not between the upper LASER level and the ground level but an intermediate level. This level relaxes fast into the ground level and thus has a low occupation. A high inversion can therefore be achieved in a four level system even by significantly weaker pumping in comparison to a three level system. This leads to a better opto-optical efficiency (ratio of output LASER power and pumping power) and reduced thermal stress in the system.

Cavities and Optical Resonators

In most LASER media the amplification factor g is not large enough to establish the wanted amplification of intensity. (1.1.2) indicates that an increase of the length of the active medium d has the same effect for the amplification as a higher g-value. The most efficient way to achieve this increase of d is the placement of the active medium in an optical resonator and thus increasing the optical path length.

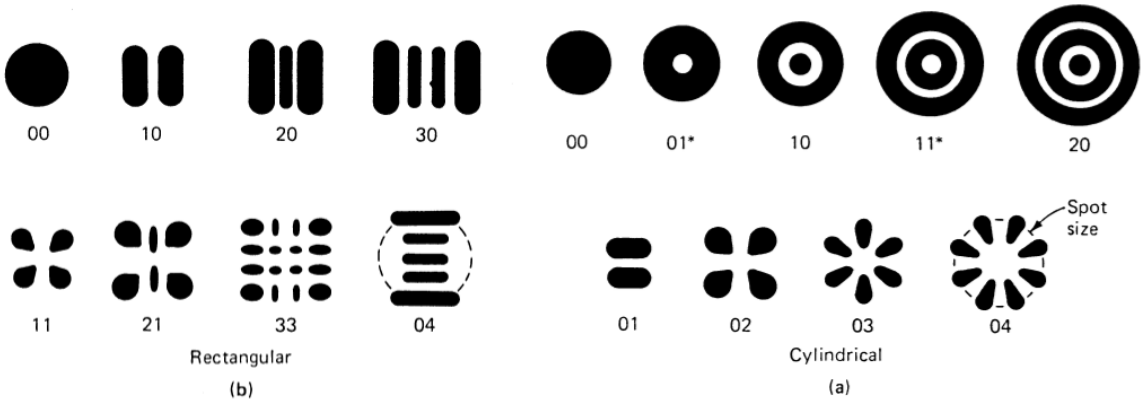

Fig. 1.3.: "Examples of (a) cylindrical and (b) rectangular transverse mode patterns. For cylindrical modes, the first subscript indicates the number of dark rings, whereas the second subscript indicates the number of dark bars across the pattern. For rectangular patterns, the two subscripts give the number of dark bars in the x- and y-directions" [2]

An optical resonator consist of two or more mirrors which are aligned in such a way that the radiation oscillate as standing wave between them. Thus the photons pass the active medium repetitively and the number of photons is increased on each round trip. In principle, open and closed cavities can be build. The closed configurations (confinement in three dimensions) are in contrast to open configurations (confinement only in one dimension) unpractical for the wavelengths in the ultraviolet, visible and near infrared spectrum [3]. Due to the fact that the reflectivity of any mirror is restricted and other losses as refraction and scattering are inevitably, the gain G must be such that all these losses are over-compensated. This leads to the LASER threshold condition

$$GRT > 1\,, \tag{1.1.3}$$

with the overall reflectivity R and the transmission T. The overall reflectivity is defined as geometric mean of the single reflectivity of all the mirror and the transmission T summarizes all losses of any kind. Usually one of the mirrors has a significantly lower reflectivity, which allows the transmission of LASER radiation. This mirror is called *output coupler* and has usually a reflectivity of 10–30% for q-switched lasers and up to 95% for continuous wave LASER (cf. 1.1.4).

Transversal modes can be determined as stable solutions of the appropriate round trip Fresnel-integrals of the resonator. These solutions are of the form of Laguerre polynomials and are denominated as *transversal electro-magnetic modes* or TEM_{xy}, where the subscript denotes the according structure in the cross section(cf. Fig. 1.3). The TEM_{00} has a Gaussian profile and is the most common profile in commercial LASER systems. This is archived by inserting an aperture into the cavity which produces large losses for any higher mode because the TEM_{00} has the smallest cross section of all modes. Longitudinal modes are defined by the number of nodes along the axis of the optical resonator. Only those modes that produce standing waves and are favored by the gain profile (cf. Fig. 1.4) can occur.

In order to manipulate the occurring transversal modes, curved mirrors can be used. However, not every combination of curvature radii $R_{1/2}$ and optical oscillator length L result in a stable configuration. The constraint for a stable system is given by the *stability criterion*

$$0 \leq g_1 g_2 \leq 1\,, \tag{1.1.4}$$

where $g_1 = 1 - L/R_1$ and $g_2 = 1 - L/R_2$ are the mirror parameters (cf. Fig. 1.5).

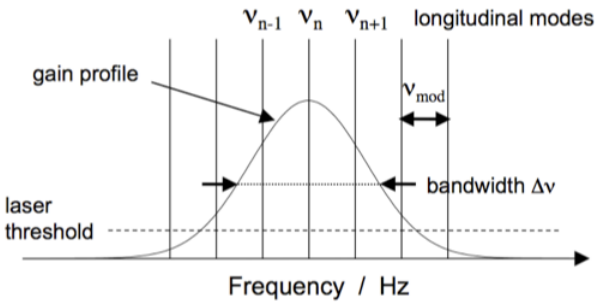

Fig. 1.4.: Gain profil and longitudinal modes. [3]

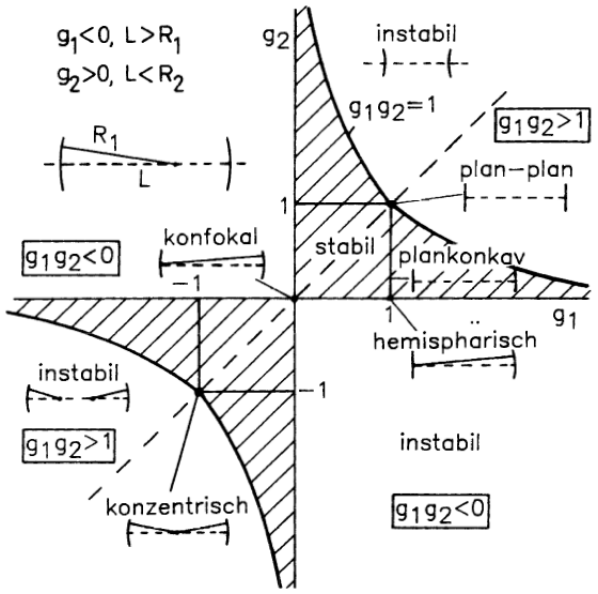

Fig. 1.5.: Stability criterion for optical resonators [1]

Pumping Nd:YAG

Yttrium aluminium garnet (YAG, $Y_3Al_5O_{12}$) doped with Neodym-Ions (Nd^{3+}) is a four level LASER medium. The term scheme is shown in Fig. 1.6. Usually, Nd:YAG is pumped at $\lambda_{pump} = 808nm$ due to its high absorption coefficient at this wavelength. However the pump band is rather narrow and thus LASER diodes (cf. 1.1.3) are far more efficient pump light sources than flash or arc lamps. Typically the ${}^4F_{3/2} \rightarrow {}^4 I_{11/2}$ transition with $\lambda_{laser} = 1064\,\text{nm}$ is used for LASER systems . Other LASER transitions occur at 1322 nm (${}^4F_{3/2} \rightarrow {}^4 I_{13/2}$) and 946 nm (${}^4F_{3/2} \rightarrow {}^4 I_{9/2}$). The lifetime of the upper LASER level ${}^4F_{3/2}$ is roughly 230 μs, which allows long pump durations (in pulsed operation mode) to create a large inversion. Together with the fast non-radiative relaxation from the pump bands into this level and from the lower LASER levels back into the ground level, leads this to a high quantum efficiency. All non-radiative transitions create lattice phonons and therefore heat and thermal stress in the crystal. Thus, at high pump powers cooling the crystal is necessary.

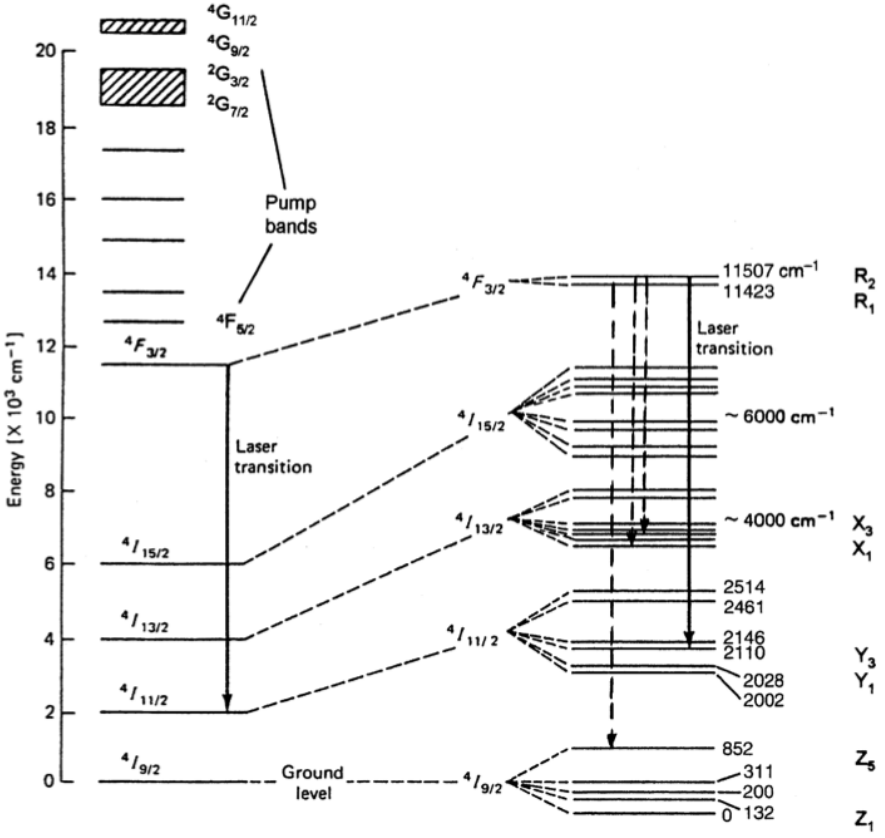

Fig. 1.6.: Term scheme of Neodym in YAG. [2]

1.1.3. LASER-diodes

In a LASER diode a pn-junction is used as the active medium. It consists of a p-type and a n-type semiconductor which are brought in contact. This leads to a diffusion of electrons in the p-type and holes in the n-type semiconductor. Thus the regions close to the contact lose their neutrality and form a space charge region. An electric field is created by this region, which opposes the process of diffusion.

The diffusion and the electric field compete with each other until a thermal equilibrium is reached. In this state, the space charge region is completely depleted of majority charge carriers.

If a voltage is applied to the pn-junction, free electrons move into the p-type and holes into the n-type semiconductor. This leads to a decrease of the depletion zone and thus a inversion of occupation number is reached in this small region. For this process the band structure of the p-type and n-type semiconductor is of importance. Discrete energy levels that follow Pauli's exclusion principle would not allow an inversion, whereas the band structure allows numerous electrons to occupy the band at slightly varying energies. If the current through the junction is high enough, electrons and holes are able to overcome the barrier formed by the depletion zone and recombine. The radiation of the recombination has the same energy as the difference between the valence and conduction band energies in the junction. For a further amplification of the emitted radiation, a cavity is needed. It is composed of two dielectric mirrors evaporated directly onto the surface of the semiconductors.

The dimension of the charge carrier region and the refractive index of the material act as waveguide directing the emitted radiation. Thus, the spatial structure of the emitted LASER radiation reflects the geometry of the charge carrier region.

Due to the fact that the energy of the band structure is depending on the density of the charge carriers and the density of the medium itself, the energy of the emitted radiation depends on the temperature of the diode and the applied current. Therefore the emission wavelength of the LASER diode is tunable in a certain range, but also requires a high accuracy when using the diode.

1.1.4. Pulse Generation and Modulation

The easiest setup for a LASER would be an active, pumped LASER medium between two mirrors. Such a device would emit continuos wave (cw) radiation if pumped continuosly or pulsed radiation if the pump light sources also operates in a pulsed mode. However, the duration of the pulsed radiation is in the order of the natural life time of the upper LASER level, i.e. . for Nd:YAG several hundred μs. If high pulse energies and intensities are needed (e.g. for spectroscopy of molecules or LIDAR applications) these pulses are far too long. The duration of the emitted LASER pulse for Nd:YAG can be shortened down to approx. $10ns$ by operating the LASER in quality-switched (q-switched) mode. This is done by reducing the quality of the resonator by such an amount, that $GRT \ll 1$ and thus no lasing can occur. Then, after creating a large inversion and thus storing huge amounts of energy in the system, the quality is rapidly increased and the stored energy is released in a short, very intense LASER pulse. In high power Nd:YAG LASERs this is usually done by a combination of polarizers, quarter wave plates and a Pockel's cell within the resonator.

In Pockel's cells, non-centrosymmetric crystals (i.e. without inversion symmetry, e.g. BBO and KDP) are used, which exhibit the Pockel's effect. This effect produces birefringence depending on an applied electric field making these crystals voltage-controlled wave plates. This effect is linear with respect to the applied electric field. Thus the angle by which the polarization is shifted can easily be adjusted by the applied voltage.

Combined with either just a polarizer or a polarizer and a quarter wave plate, a Pockel's cell can be used as fast optical switch.

The first combination uses the Pockel's cell as a half wave plate, if the half wave voltage $U_{\lambda/2}$ is applied. Appropriately aligned, no photons can pass this analyzer-polarizer combination as long as this voltage is turned on. If the voltage is turned off, the polarization is not shifted anymore and oscillations start to build up. After a short build-up time a very intense laser pulse is emitted, which contains most of the energy previously stored by pumping. However, for most crystals $U_{\lambda/2}$ is very large usually in the order of many kV and thus is difficult to switch on or off in short times as required by q-switching.

Thus, because $U_{\lambda/2} = 2 \cdot U_{\lambda/4}$ counts, Pockel's cell are usually used as quarter wave plates. This is done by placing into the cavity in front of the rear, high reflecting mirror a quarter wave plate, a Pockel's cell and a polarizer in this order. Because the quarter wave plate is placed directly in front of the rear mirror and every photon must pass it twice before passing any other component it acts as

effective half wave plate. Thus, the oscillator is blocked, because the total wave shift is 90°. If the quarter wave voltage $U_{\lambda/4}$ is applied to the Pockel's cell, which is placed between the quarter wave plate and the polarizer, the total wave shift sums up to 180°. Therefore oscillations can build up which leads to a very intense LASER pulse.

The repetition rate in q-switched operation can be adjusted by the modulation of the applied voltage.

1.2. Second Harmonic Generation as Nonlinear Optical Effect

In order to obtain wavelength that are not emitted from the active LASER medium, non-linear optical effects can be used to produce the desired wavelength. Thus the advantage of solid state LASERs (e.g. high average output power) can also be achieved at these wavelengths.

The electrical polarization, which is a measure for the radiation emitted by an atom, is given as

$$\vec{P}_{el} = \epsilon_0 \left(\chi_1 \vec{E} + \chi_2 \vec{E}^2 + \ldots \right), \tag{1.2.1}$$

however the non-linear optical susceptibility χ_2 only occurs in an-isotropical materials [1]. If two plain waves interfere with each other inside a non-centrosymetric crystal energy and momentum conservation yield

$$\omega_{res} = \omega_1 \pm \omega_2, 2\omega_1, 2\omega_2 \tag{1.2.2}$$

$$\vec{k}_{res} = \vec{k}_1 \pm \vec{k}_2, 2\vec{k}_1, 2\vec{k}_2 \,. \tag{1.2.3}$$

Thus, if one plain wave with frequency ω_1 is irradiated into the crystal, the wave can interfere with itself creating a second wave oscillating with the frequency $\omega_{sh} = 2\omega_1$ and wave vector $\vec{k}_{sh} = 2\vec{k}_1$ due to the non-linear part of the polarization. Due to momentum conservation counts

$$|2\vec{k}_1| = |\vec{k}_{sh}| \Leftrightarrow 2n_1\omega_1 = n_2\omega_{sh} \,. \tag{1.2.4}$$

In an birefringent crystal this can be fulfilled if the waves are accordingly polarized, because the crystal has different refractive indices in the ordinary and extraordinary axes. To achieve the required phase matching condition, i.e. $n_1 = n_2$, the crystal must be aligned in the appropriate angle which can be determined by the refractive index ellipsoid (cf. Fig. 1.7). Note, that these effect is of second order with respect to the electromagnetic field intensity and thus high intensities are required. With higher intensities even higher harmonics can be generated.

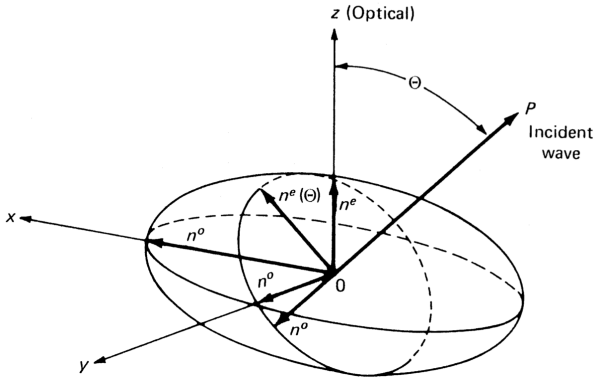

Fig. 1.7.: "Indicatrix ellipsoid of a uniaxial crystal. Also shown is a cross section perpendicular to the light propagation direction P." [2]

2. Experimental Setup and Procedure

2.1. Experimental Setup

A sketch of the experimental setup can be found in Fig. 2.1. It consists of a Laser diode with two lenses (the first for collimating the beam and a second one for focusing it into the rod) for pumping. The cavity itself consists of two elements. First the Nd:YAG rod with a diameter of approx. 3 mm and an length of approx. 10 mm of unknown doping. The side facing the pump diode is HR-coated for a center wavelength of 1064 nm. Second, a curved mirror with curvature radius $r = 100\,\text{mm}$, which is used as output coupler. During operation at 1064 nm the output coupler has a coating with reflectivity of $R \approx 2\%$ at center wavelength 1064 nm. For second harmonic generation an output coupler with a high reflective coating at center wavelength 1064 nm and a high transmission at center wavelength 532 nm is used.

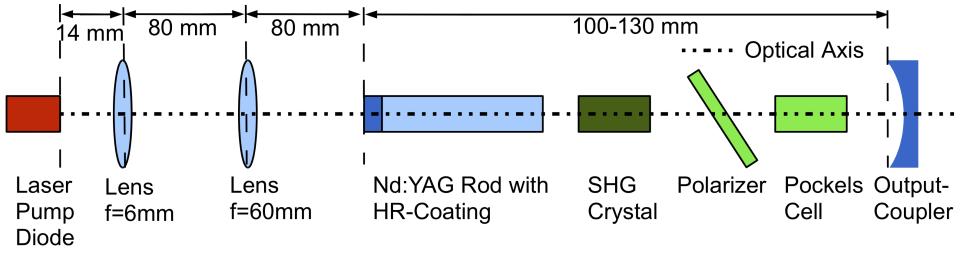

Fig. 2.1.: Experimental setup: Collimation and focusing of pump diode Laser and laser cavity in q-switched second harmonic generation operation.

The length of the cavity, i.e. the distance between the two mirrors, was changed during the experiment as was the number of components inside the cavity whereas the distances between pump diode Laser , the lenses and the rod were fixed. During cw-operation at 1064 nm only an adjustable aperture was inside the cavity, whereas during second harmonic generation the aperture was replaced by a SHG crystal (Potassium titanyl phosphate, KTP, $KTiOPO_4$). In q-switched operation a Pockel's cell with a polarizer (quartz disc aligned at Brewster's angle ($\approx 57°$)) was inserted and therefore the cavity had to be slightly enlarged.

The output power of the Laser was measured with a powermeter and a CMOS-chip as well while the beam profile was recorded with a CCD-camera. During measurements with CMOS-chip and CCD-Camera ND- and high/low-pass filters were applied if necessary.

All components were mounted on an slide rail for z-adjustment and inside adjustment mounts for x-y- and angle-alignment.

2.2. Experimental Procedure

The emission of the pump Laser diode was characterized. The output power was measured at different currents and temperatures at a center wavelength of 808 nm. Pumping the rod at 808 nm was chosen because the absorption coefficient of Nd:YAG is maximal at this wavelength (cf. Fig. 2.2). The emitted beam at 808 nm was collimated and then focused into the rod. The rod and the output coupler were aligned parallel to the optical axes and the thusly constructed cavity was aligned for maximal output

power. The adjustable aperture was then build into the cavity and adjusted such, that the output power was maximal while the transmitted beam profile was TEM_{00}.

The beam profile was recorded with different transmitted modes, which were selected by adjusting the output coupler and the aperture. With a computer the recorded black/white-images were transformed to false color images.

The CMOS-chip was calibrated by fitting the measured voltage against the output power measured by the powermeter. This was performed at 1064 nm and 532 nm separately. Due to its' higher sensitivity the CMOS-chip was used to measure the quantum efficiency and determine the LASER threshold.

To operate in second harmonic generation the output coupler was changed and the aperture was replaced by an KTP crystal as already mentioned in 2.1. The crystal has a dimension of approx. $3 \times 3 \times 9$ mm. The crystal was aligned such, that output power at 532 nm was maximal. Two different positions of the crystal were used. One was with the crystal immediately in front of the output coupler and the other with the crystal in front of the rod in vicinity to the focus of the output coupler.

To operate the LASER in q-switched mode the Pockel's cell and polarizer were built into the cavity as sketched in Fig. 2.1 and aligned for maximal output power. The repetition rate was set via a frequency generator, which triggered the high voltage supply for the Pockel's cell and simultaneous a PC-oscilloscope. The LASER pulses were measured with the calibrated CMOS-chip connected to the PC-oscilloscope while output power was measured with both CMOS-chip and power meter.

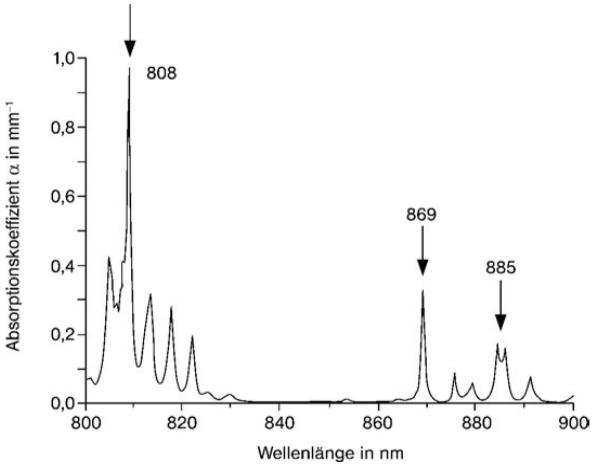

Fig. 2.2.: Absorptions bands and coefficients of Nd:YAG [1]

3. Experimental Results and Analysis

3.1. Characterization of Diode Pump Laser at Central Wavelength 808 nm

The dependence of the diode's emitted wavelength in dependence on temperature and current were taken from [3]. However, this was only available for only three different currents (200 A, 350 A and 500 A). Thus, only for this current/temperature-values the emitted wavelength is known to be 808nm. Using the provided characterization curves one can determine that lower diode temperatures lead to shorter wavelengths of the emitted radiation. Fig. 2.2 shows clearly, that the absorption in Nd:YAG for shorter wavelengths than 808 nm is higher than for longer ones. For this reason, for measuring in the range of 100 – 200 A diode current a temperature of 36.3°C was used, which gives at a current of 200 A a known wavelength of 808 nm and shorter wavelengths for smaller currents. The resulting diode power $\mathrm{P_{diode}}$ over diode current $\mathrm{I_{diode}}$ curve could be determined to be

$$P_{\mathrm{diode}} = (0,99 \pm 0,01)\frac{\mathrm{mW}}{\mathrm{A}} I_{\mathrm{diode}} - (151 \pm 1)\mathrm{mW}\,, \tag{3.1.1}$$

which is also show in Fig. 3.1.

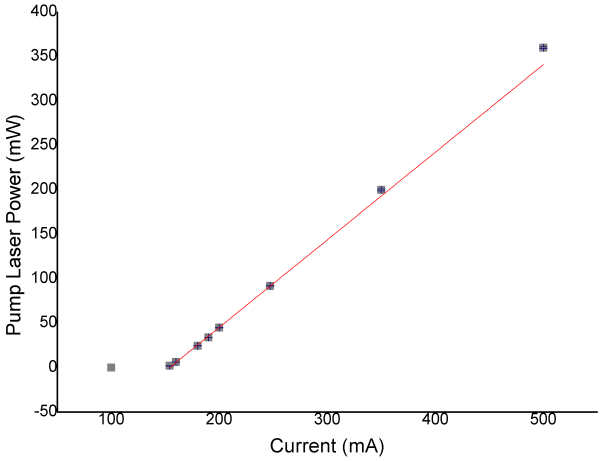

Fig. 3.1.: Diode characterization: diode output power P_{diode} over diode current I_{diode}.

3.2. Calibration of the CMOS-chip at 532 nm and 1064 nm

For the calibration of the CMOS-chip the Laser output power was adjusted by manipulating the applied current. The output power was measured with an RG1000 filter to avoid corruption due to the radiation emitted by the pump diode. To avoid the saturation of the CMOS-chip, a set of neutral density filters were chosen such that at the highest output power the CMOS-chip was not in the range of saturation. This combination of ND and RG filters was not changed during the measurement as it would alter the calibration. During the measurements with the power meter no filters except the RG1000 filter were applied. The resulting calibration curve is

$$\mathrm{P_{out}} = (0.030 \pm 0.001)\frac{\mathrm{mW}}{\mathrm{mV}} U_{\mathrm{CMOS}} - (0.50 \pm 0.02)\mathrm{mW}\,, \tag{3.2.1}$$

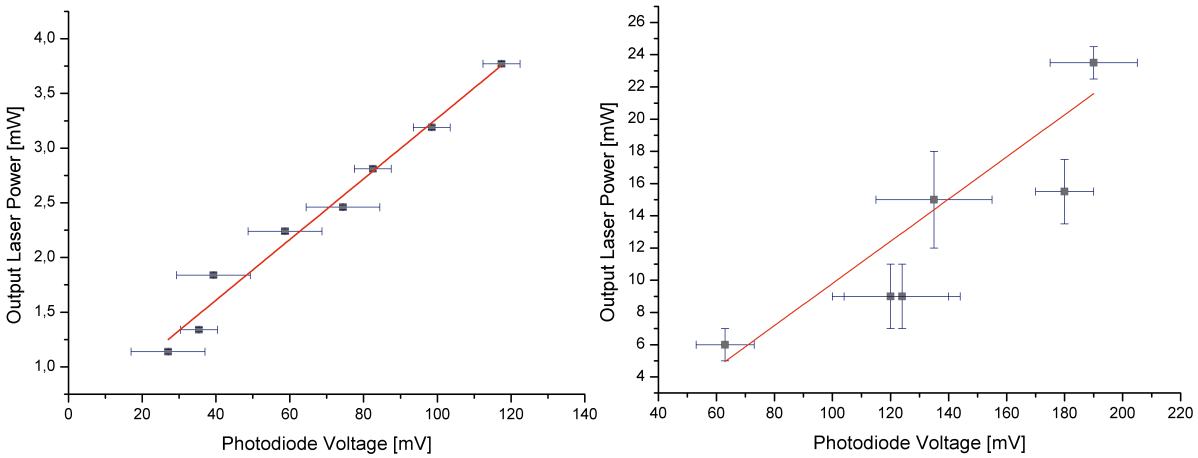

Fig. 3.2.: Calibration of CMOS-chip at 1064 nm (left) and 532 nm (right): LASER output power P_{out} over voltage U_{CMOS}.

which is shown in Fig. 3.2.

The calibration was also performed at 532 nm. A RG1000 filter had to be applied as before due to pump LASER light. However, the available filters also decreased the power at 532 nm significantly. Furthermore, the frequency conversion was very unstable and thus the emitted power had large fluctuations. This fluctuations in combination with the very high sensitivity of the CMOS-chip and the low overall intensity caused errors in the range of 50% of the measured voltage. Therefore, an analysis of this data was omitted. The power detector did not show this fluctuation due to its lower sensitivity and was therefore used to measure the output power during 532nm-operation.

3.3. Operation at 1064 nm (cw)

Assuming that the rear cavity mirror is flat (i.e. $R \to \infty$) and the output coupler is curved with $R = 100\,\text{mm}$ the stability criterion (1.1.4) states, that for a stable configuration the cavity length L must be $0 \leq L \leq 100\,\text{mm}$. For the continuous wave operation at 1064 nm we realized at total cavity length of 100 mm.

The LASER output power in dependence on the diode power at a defined wavelength of 808 nm was measured. However, as already mentioned, this could only be done for three different values due to the lack of characterization curves. The results are summarized in Tab. 3.1. The intracavity power is calculated via $P_{intra} = (1+R)/(1-R) \cdot P_{out}$, where P_{out} denotes the LASER output power and R the reflectivity of the output coupler. The opto-optical efficiency η_{oo} is calculated as ratio of output LASER power and diode power $\eta_{oo} = P_{out}/P_{diode}$.

T_{diode} | °C	I_{diode} | mA	P_{diode} | mW	P_{out} | mW	P_{intra} | mW	η_{oo}
36.3	200	44.9 ± 0.1	1.5 ± 0.1	150 ± 10	0.033 ± 0.002
35.8	350	200 ± 1	2.5 ± 0.1	240 ± 10	0.013 ± 0.001
33.7	500	316 ± 1	4.0 ± 0.2	400 ± 13	0.013 ± 0.001

Tab. 3.1.: Summery of measured LASER parameters in cw-operation at 1064 nm

This data however is not enough to observe or extrapolate a reasonable LASER threshold. In fact, an extrapolation yields a threshold of $P_{diode} = -111\text{mW}$ which is nonsense. If the data point for the

lowest pump power is omitted, the threshold becomes 12 mW. Thus we used the data recorded at the calibration of the CMOS chip to extrapolate a threshold in terms of diode current and determined the threshold pump power via (3.1.1). We find $I_{threshold} = 240\text{mA}$ or $P_{threshold} \approx 100\text{mW}$. However, as already discussed, the wavelength of the pump LASER diode changed as a function of temperature, which accounts for the large error margin and furthermore we observed LASER radiation at $P_{diode} = 44,9\,\text{mW}$. Thus, we assume, that the LASER threshold is in the range of 10–50 mW

The slope efficiency of the LASER output power determined using the same set of date is

$$\eta_{slope} = (0.010 \pm 0.001)\,. \tag{3.3.1}$$

Thus, the slope efficiency is consistent with the efficiency determined in Tab. 3.1.

To alter the transversal LASER modes of the emitted radiation the aperture and the alignment of the output coupler were adjusted. The beam profile was recorded with the CCD-camera. Four different modes are shown in Fig. 3.3 and a detailed analysis of these modes can be found in Appendix A.

Fig. 3.3.: Color inverted black-white images of observed transversal modes taken with a CCD-camera: (from left to right) TEM_{00}, TEM_{01}, TEM_{14} and a superposition of TEM_{02} and TEM_{00}.

3.4. Operation at 532 nm (cw and q-switched)

3.4.1. CW-Operation

As already mentioned, the cavity had to be enlarged by 30 mm to contain all required components. Therefore, the configuration become unstable thus resulting in a smaller gain of this configuration compared to the stable configuration due to walk-off losses [2]. Instead of the aperture, a KTP crystal was inserted with a free aperture of $\approx 3\text{mm}$.

If the KTP crystal was placed in front of the output coupler instead of placing it in the vicinity of the focus, the conversion efficiency decreased significantly (cf. Tab. 3.2, 3.3). This can be explained rather easily. It is valid to assume, that on the surface of the curved mirror, the beam diameter is in the order of the diameter of the output coupler. Thus, the intensity in the vicinity of the output coupler is several orders of magnitude smaller than in the vicinity of the focus, because intensity scales with the second order of beam diameter. Furthermore, the beam diameter at this position is larger than the free aperture of the crystal and therefore only a fraction of the total power can be used. Thus, in the further course of the experiment, the crystal was aligned such that the focus of the output coupler was in the vicinity of the the crystal surface facing the Nd:YAG-rod but still inside the crystal.

To calculate the efficiency of the intracavity second harmonic generation we assumed the same intracavity power at 1064 nm as during the operation at 1064 nm. Due to the high reflectivity of the output coupler this is a good approximation, because the systematic errors caused by this approximation (approx. 2%) are lower than the achieved measuring accuracy.

T_{diode} / °C	I_{diode} / mA	P_{diode} / mW	P_{out} / mW	$P_{intra,IR}$ / mW	η_{SHG}
36.3	200	44.9 ± 0.1	3 ± 2	150 ± 10	0.02 ± 0.01
35.8	350	200 ± 1	14 ± 1	240 ± 10	0.056 ± 0.005
33.7	500	316 ± 1	22 ± 1	400 ± 13	0.055 ± 0.003

Tab. 3.2.: Summery of measured Laser parameters in cw-operation at 532 nm close to the Nd:YAG rod.

T_{diode} / °C	I_{diode} / mA	P_{diode} / mW	P_{out} / mW	$P_{intra,IR}$ / mW	η_{SHG}
36.3	200	44.9 ± 0.1	3 ± 1	150 ± 10	0.019 ± 0.007
35.8	350	200 ± 1	2.0 ± 0.5	240 ± 10	0.008 ± 0.003

Tab. 3.3.: Summery of measured Laser parameters in cw-operation at 532 nm close to the output coupler.

3.4.2. Q-Switched Operation

To operate in q-switched mode a Pockel's cell was inserted into the cavity as shown in Fig. 2.1 and aligned at maximal output power. The output power was measured with the power meter and the emitted pulse trains were observed via the CMOS-chip and the PC-Oscilloscope which was triggered from the same source (frequency generator) as the high voltage supply of the Pockel's cell. The Hold-off of the Pockel's cell was determined by adjusting the high voltage of the Pockel's cell during cw-operation. However, both, the CMOS-Chip and the powermeter could not determine a change in output power although a significant change of the brightness of the Laser beam could be observed at a controller reading of 8.7 kV. This voltage was used during q-switched operation.

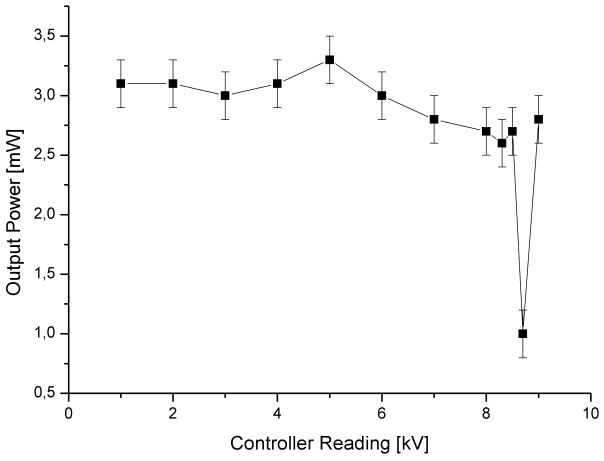

Fig. 3.4.: Hold-off voltage of Pockel's Cell. The data point at 8.7 kV was inserted manually for the sake of plotting.

The Pockel's cell and the output coupler were then aligned such, that the Laser operated in q-switched mode. It could be observed, that wether the cavity was q-switched or not depends of the alignment of the output coupler with respect to the Pockel's cell. This can be explained by the different angles between fast and slow axes of the Pockel's cell crystal and the optical axis and the propagating Laser beam respectively and thus the dependence of refraction indices for fast and slow rays on this alignment (cf. Fig. 1.7).

The pulse train emitted from the LASER is shown in Fig. 3.5. We determined a pulse time spacing of 24.4 ms which corresponds to a repetition rate $f_{rep} = 41\,\text{Hz}$. A output power of $P_{out} = 3\text{mW}$ was measured at this repetition rate using a pump current of 500 mA. This yields a pulse power of $P_{pulse} = 7,3 \cdot 10^{-5}\text{W}$ and a pulse energy of $E_{pulse} = 7,3 \cdot 10^{-5}\text{J}$ respectively. In Fig. 3.6 a single LASER pulse with two different time scales is shown. Using this figures a FWHM pulse duration of $\tau_{pulse} \approx 0,35\text{ms}$ and a rise time of $\tau_{rise} = 1\mu\text{s}$ and a fall time of $\tau_{fall} = 1\text{ms}$ could be determined. However, considering the pulse time shapes it was obvious that the input impedance of the PC-oscilloscope is far to high (presumably 1 MΩ) which caused an elongation and distortion of the pulse time shape. The pulse form should be more like a gaussian with a FWHM duration of 10–25 ns and thus a rise and fall time of same order of magnitude [2]. A adjustment of the input impedance was however not possible.

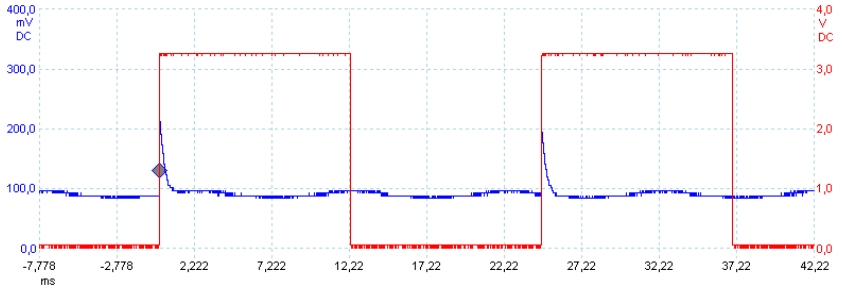

Fig. 3.5.: Emitted pulse train recorded with CMOS-chip (blue) and trigger pulse (red) in q-switched operation at 532nm.

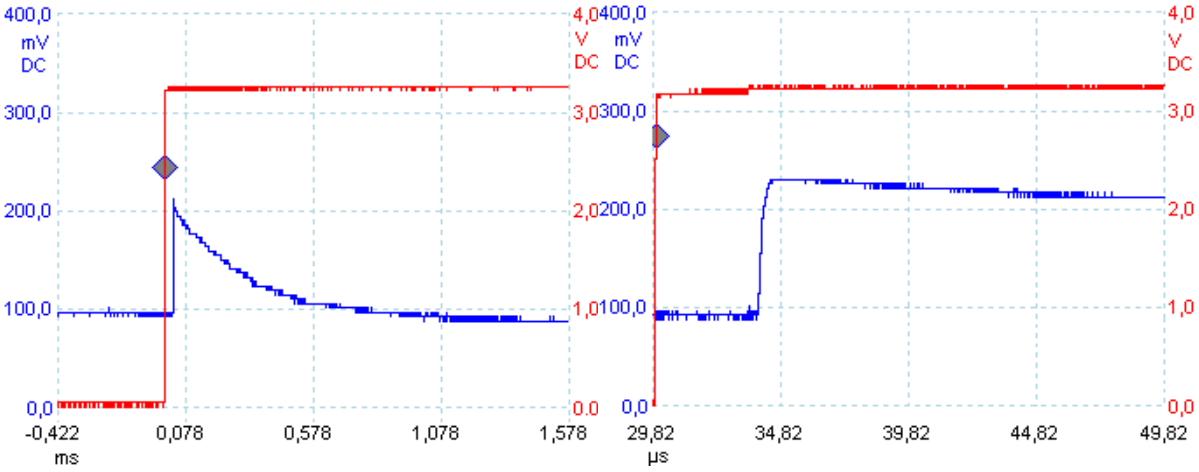

Fig. 3.6.: Single LASER pulse (blue) and trigger single (red) at different time scales

4. Conclusion

A diode pumped solid state LASER was successfully built and operated, in continuous wave operation at 1064 nm and in q-switched and continuous wave operation with intracavity second harmonic generation (output wave length 532 nm).

Several different beam profiles (transversal electromagnetic modes) were observed and recorded with a CCD-Camera during cw-operation at 1064 nm. We were able to identify these modes as Gauss-Hermitian and Laguerre-Gaussian polynomials and determined the relevant parameters (relative beam waist, relative peak intensity and coefficients l,p and m,n respectively) by numerical simulation.

The laser threshold could not be determined exactly but an interval could be ascertained. We found, that the LASER threshold must be between a pump power of 10 mW and 50 mW.

During intracavity second harmonic generation we determined the conversion efficiency for two different setups, with the KTP-crystal in front the rod or in front of the output coupler. We observed, that the efficiency of the setup with the crystal in front of the rod and consequently in the focus of the curved mirror was a order of magnitude higher than for the setup with the crystal in front of the mirror. This can be explained by the spatial distribution of radiation intensity along the optical axis. Furthermore, the output power at 532 nm was an order of magnitude higher than in cw-operation at 1064 nm with same pump parameters. We found the conversion efficiency to be approx. 5% while the opto-optical efficiency during cw-operation at 1064 nm was approx. 1%. This is due to the fact, that the infrared intracavity power which generates the second harmonic is a factor 50 higher than the output power in cw-operation at 1064 nm which leads to a high output power at 532 nm.

Furthermore, using a Pockel's cell q-switched operation was performed at 532 nm. We observed the pulse time shape and duration as well as the repetition rate via the CMOS-chip and an PC-oscilloscope. However, due to the high input impedance of the oscilloscope, we could not acquire reasonable data neither for pulse duration nor rise and fall times. The time averaged output power during q-switched operation was as high as during cw-operation at 1064 nm while the power during cw-operation at 532 nm was a order of magnitude higher. This could be improved by a more precise alignment.

Bibliography

[1] Eichler, Jürgen; Eichler, Hans J.; *Laser*; 3rd Edition; Springer-Verlag Berlin Heidelberg New York; 1998

[2] Koechner, Walter; *Solid State Laser Engineering*; Springer Series in Optical Sciences; 6th Edition; Springer Science+Business Media, Inc.; 2006

[3] *Ma 14 - Solid State Laser Principles*; Instructions for the Advanced Laboratory Course at Freie Universität Berlin; 2011

A. Analysis of observed transversal LASER modes

Transversal LASER modes can be described - depending on the design of the cavity - by Hermite-Gaussian or Laguerre-Gaussian modes. The later occur if the cavity is cylindrically symmetric, the first if no radially symmetry exists. The intensity distribution of the beam perpendicular to the direction of propagation z is given by

$$I_{pl}(r,\Phi,z) = I_0\rho^l \left[L_p^l(\rho)\right]^2 \left(\cos^2 l\Phi\right) \exp(-\rho) \tag{A.0.1}$$

for Laguerre-Gaussian modes, where $\rho = 2r^2(z)/w^2(z)$ with the beam waist $w(z)$ and L_p^l is the generalized Laguerre polynomial of order p and index l. For Hermite-Gaussian modes the intensity is given by

$$I_{mn}(x,y,z) = I_0 \left[H_m\left(\frac{x\sqrt{2}}{w(z)}\right)\exp\left(-\frac{x^2}{w^2(z)}\right)\right]^2 \left[H_n\left(\frac{y\sqrt{2}}{w(z)}\right)\exp\left(-\frac{y^2}{w^2(z)}\right)\right]^2 \tag{A.0.2}$$

with the Hermite polynomials H_m and H_n [2].

To analyse the obtained TEMs, the detected 8-bit gray scale from the CCD camera was converted and distinct cross sections along the x-axis were analyzed by numeric simulation using A.0.1 and A.0.2 respectively. A fit of the parameters p and l or m and n respectively led to the determination of the actual mode and its designation. For each of the four detected modes a false color image and the cross section are shown. Both as well from the experimental data and the numerical simulation. The numerical simulation was performed in MATHEMATICA.

A.1. Laguerre-Gaussian TEM_{00}

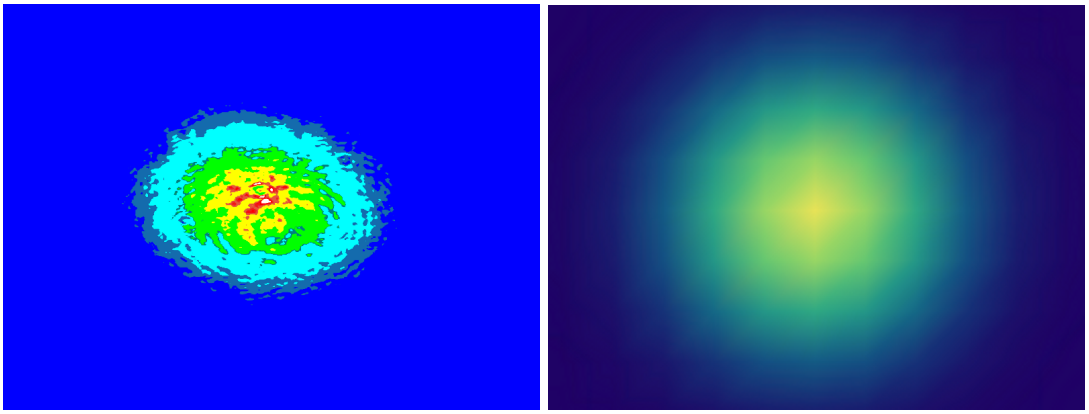

Fig. A.1.: False color image of TEM_{00} from experimental data (left) and numerical simulation (right)

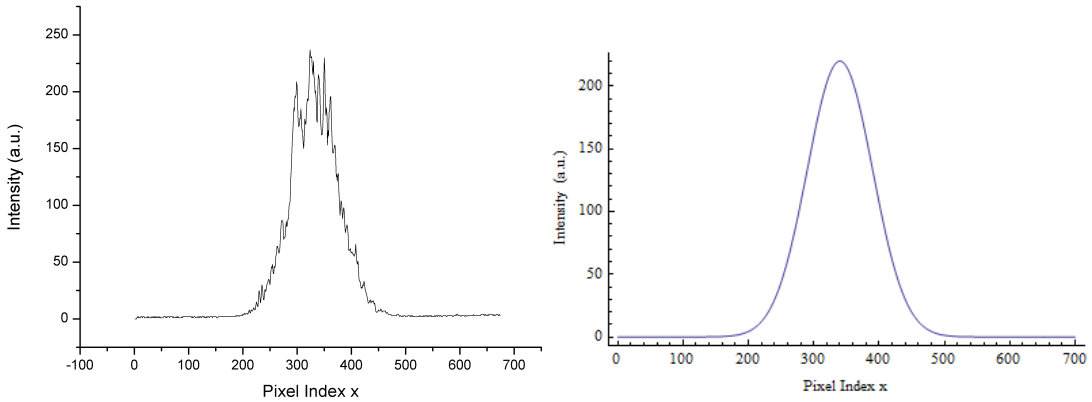

Fig. A.2.: Cross section of TEM_{00} from experimental data (left) and numerical simulation (right)

The TEM_{00} mode was fitted with Laguerre-Gaussian with an intensity $I_0 = 220$, a shift of the origin by 340 Px and a beam waist of 100 Px at an angle $\Phi = 0°$.

A.2. Laguerre-Gaussian TEM_{01}

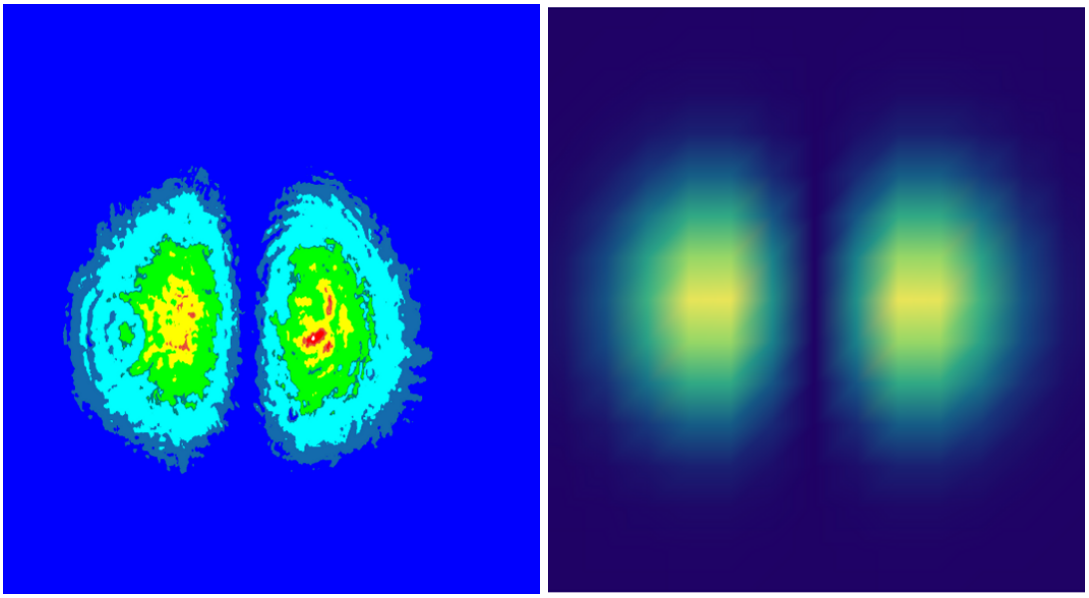

Fig. A.3.: False color image of TEM_{01} from experimental data (left) and numerical simulation (right)

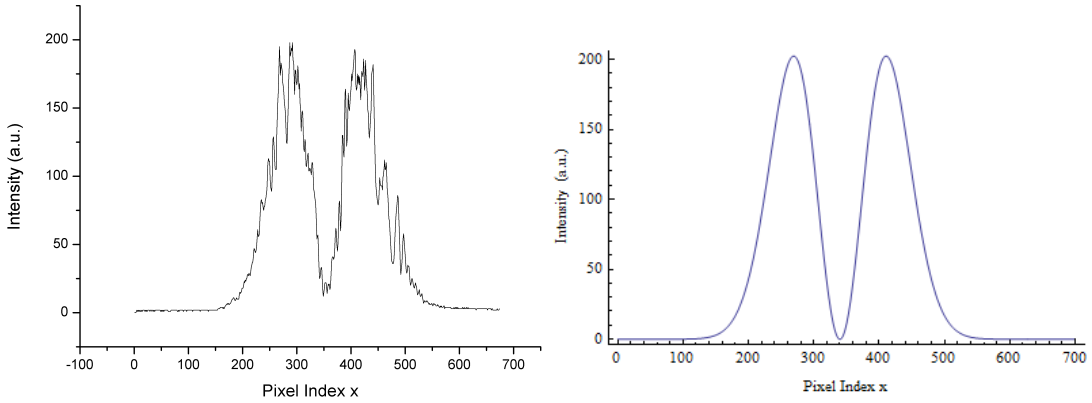

Fig. A.4.: Cross section of TEM_{01} from experimental data (left) and numerical simulation (right)

The TEM_{01} mode was fitted with Laguerre-Gaussian with an intensity $I_0 = 550$, a shift of the origin by 340 Px and a beam waist of 100 Px at an angle $\Phi = 0°$.

A.3. Laguerre-Gaussian $\mathrm{TEM}_{02} + \mathrm{TEM}_{00}$

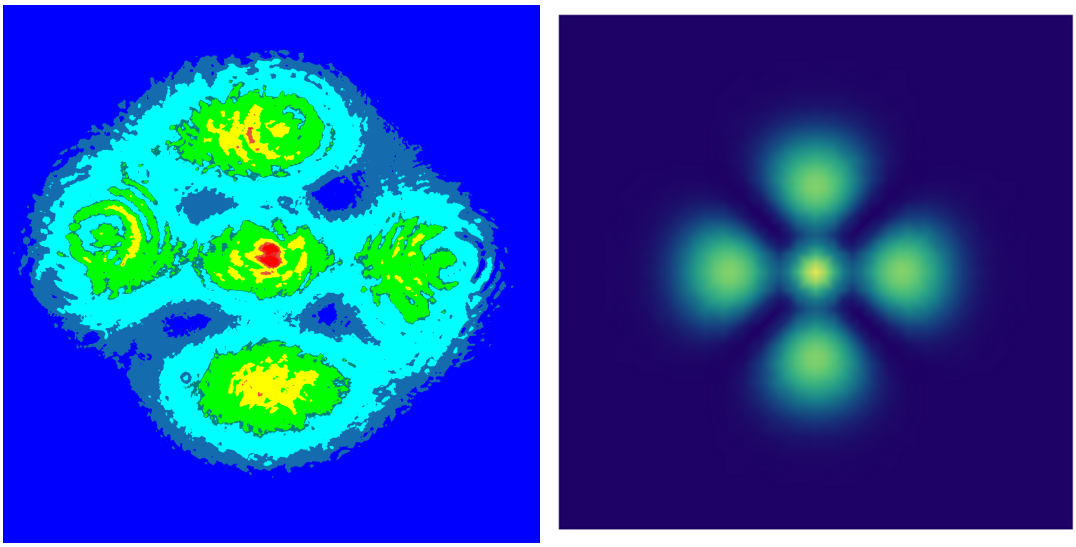

Fig. A.5.: False color image of $\mathrm{TEM}_{02} + \mathrm{TEM}_{00}$ from experimental data (left) and numerical simulation (right)

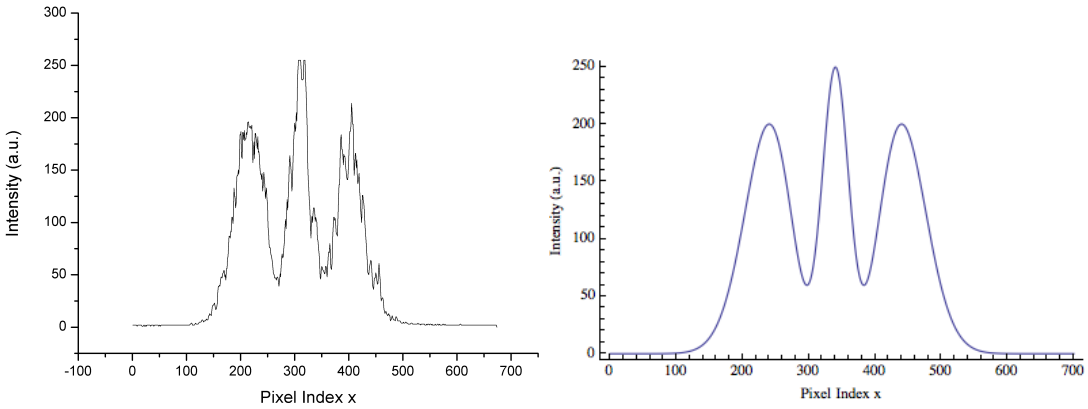

Fig. A.6.: Cross section of $\mathrm{TEM}_{02} + \mathrm{TEM}_{00}$ from experimental data (left) and numerical simulation (right)

The $\mathrm{TEM}_{02} + \mathrm{TEM}_{00}$ mode was fitted with Laguerre-Gaussian as a superposition of TEM_{02} and TEM_{00} with an intensity $I_0 = 370$ for TEM_{02} and $I_0 = 250$ for TEM_{00}, a shift of the origin by 340 Px and a beam waist of 100 Px for TEM_{02} and 40 Px for TEM_{00} at an angle $\Phi = 0°$.

A.4. Hermite-Gaussian TEM_{14}

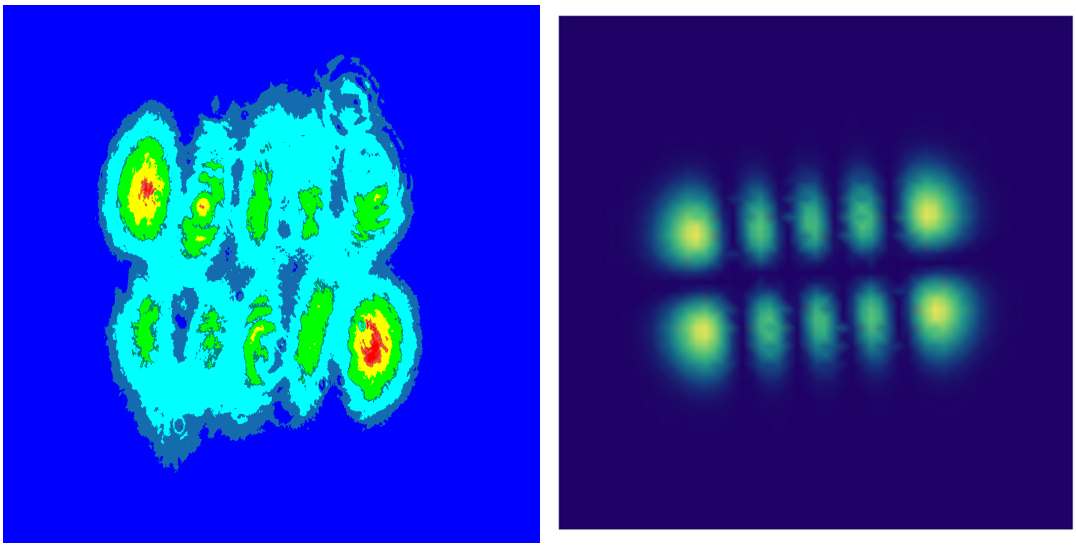

Fig. A.7.: False color image of TEM_{14} from experimental data (left) and numerical simulation (right)

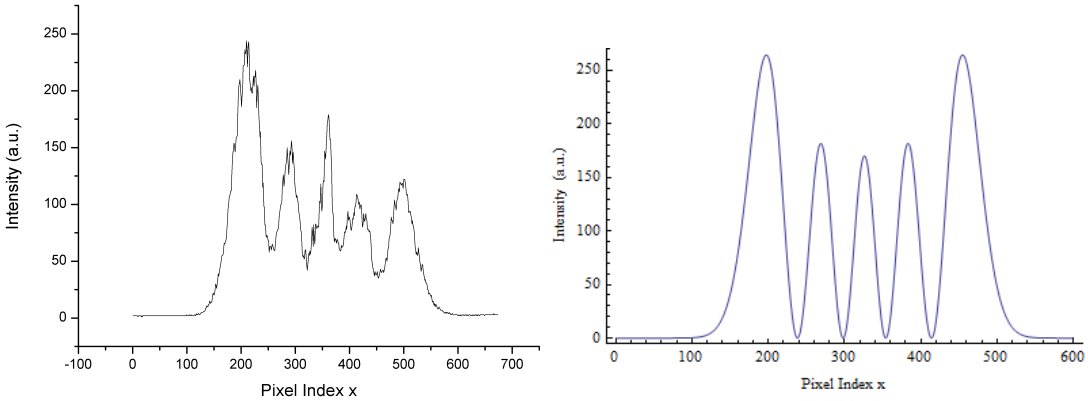

Fig. A.8.: Cross section of TEM_{14} from experimental data (left) and numerical simulation (right)

The TEM_{14} mode was fitted with Hermite-Gaussian with an intensity $I_0 = 4$, a shift of the origin by 300 Px and a beam waist of 75 Px. For better comparison with the experimental data, the numerical plot was tilted by 5°.